The Self-Scattering of the Compton Recoil Electrons Produced by Co^{60} Gamma-Rays

By

Tunahiko SIDEI, Takenobu HIGASIMURA and Katuhiro KINOSITA

Department of Applied Physics

(Received August 31, 1956)

When γ-rays penetrate through a matter, electrons are ejected by the three processes: the photoelectric effect, the Compton effect, and the pair creation. Suffering multiple scattering and degrading its energy, the secondary electrons ejected by the photon pass some distance in the matter. If the scatterer is a thin layer, some of the electrons penetrate it. It is difficult to calculate the energy spectrum and the angular distribution of penetrated electrons, because this process is very complicated. But, since the problems of the efficiency of *G-M* counter for the γ-ray, the back-scattering and the self-scattering of the β-ray belong to this process, it is important to study the phenomena by various ways.

Concerning the efficiency of the *G-M* counter for γ-rays, many works were done since about 1930,[1] but they were only for γ-rays of a few certain energies because γ-rays of natural radioactive elements, such as *Ra* and *ThC'*, were used for most of the early measurements. In these days, the *G-M* counter became to be less important as the detector of γ-rays in the field of nuclear physics; however, on the other hand, the utilization of radioactive isotopes has extended into various fields of science and technology and it has become important to clarify the dependence of its efficiency on the energy of γ-rays. Some measurements have been conducted in a wide energy region in the last ten years.[2) 3) 4)] Also, some fundamental data were obtained for the back-scattering and self-scatteing of β-rays.[5)] As a way to study these phenomena—the process by which the multiple-scattering of the electron became mixed with the degradation of its energy—we measured the self-scattering of the secondary electrons by the γ-rays of Co^{60} and obtained the results which are explained hereinafter.

I. The Angular Distribution

Experimental Procedure

The geometry of our measurement is shown schematically in Fig. 1. A collimated

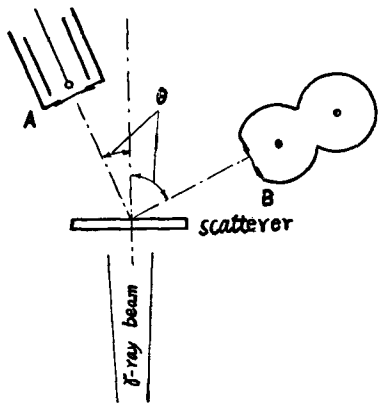

Fig. 1. Schematic drawing of the experimental arrangement.

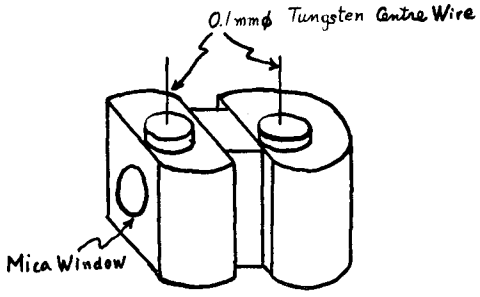

Fig. 2. Dual counter.

γ-ray beam of Co^{60} is applied perpendicularly on the sample (scatterer) and the emergent electrons are detected at each scattering angle θ by the *G-M* counter A and B. Electrons ejected from the container of the source or the layer of the air along the path of the ray can be removed from the incident beam by the magnetic field of a electromagnet. The counter A is a usual end-window counter with a mica window of 2.2 cm in diameter and of 1.82 mg/cm^2 in thickness. The distance from the scatterer to the front surface of its counting volume is 3.7 cm. A is used to measure the intensity of the emergent electrons at the scattering angle $\theta = 0°$, 12.5°, 25°. At the position where θ is larger than 25°, the background counting rate is very large on account of the leakage of the γ-ray and the standard deviation of the measurement becomes larger. Therefore, we produced a dual counter B to avoid this disadvantage. It consists of two *G-M* counters joined together which has a thin aluminium foil (1.68 mg/cm^2 in thickness) between them as shown in Fig. 2. The thickness of the mica window of the forward counter is 4.1 mg/cm^2 and its diameter, 1.5 cm and the distance from the mica window to the scatterer, 3.7 cm. As the main background count are due to the electrons ejected from the wall by the leaked γ-ray, and these electrons have scarecely a chance to penetrate both counters, the background counting rate will be reduced remarkably when coincidence counts are taken. By this technique our measurements were easily carried out at the scattering angle of $\theta = 25°$, 45°, 65°, 115°, 135° in the relatively high γ-ray field. The curves in Fig. 6 are connected at $\theta = 25°$ by the data obtained by the two methods.

Results Obtained

Relations of the number of the emergent electrons with the thickness of the scatterer are shown in Figs. 3, 4 and 5. Assuming the usual self-scattering formula of the β-rays to be approximately

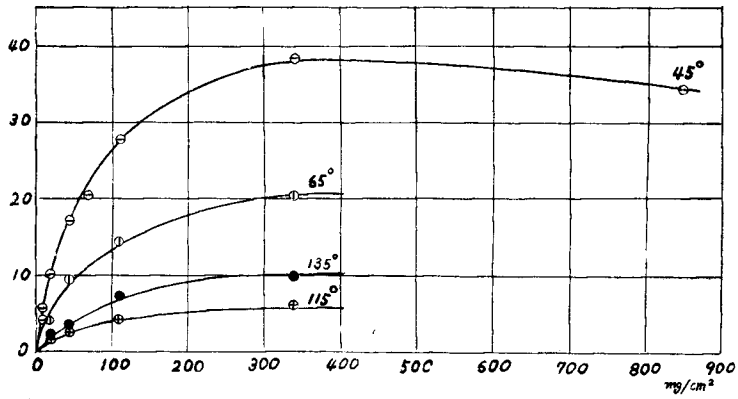

Fig. 3. Relations between the intensity of emergent electrons and the thickness of silver scatterers at each scattering angle shown. The ordinate is in the arbitrary scale.

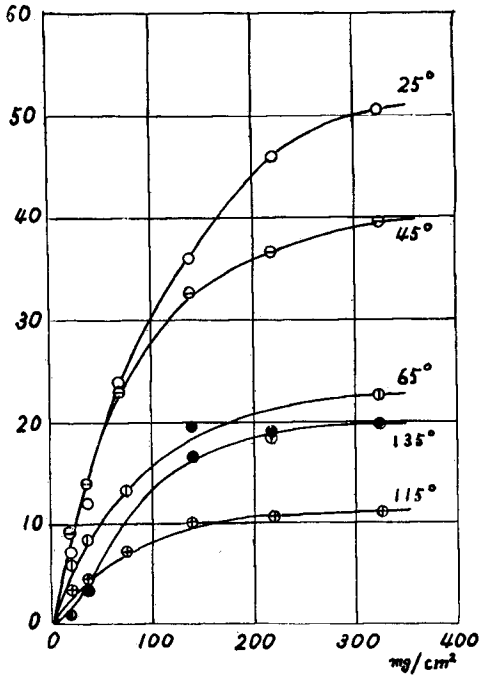

Fig. 4. Relations between the intensity of emergent electrons and the thickness of lead scatterers at each scattering angle shown. The ordinate is in the arbitrary scale.

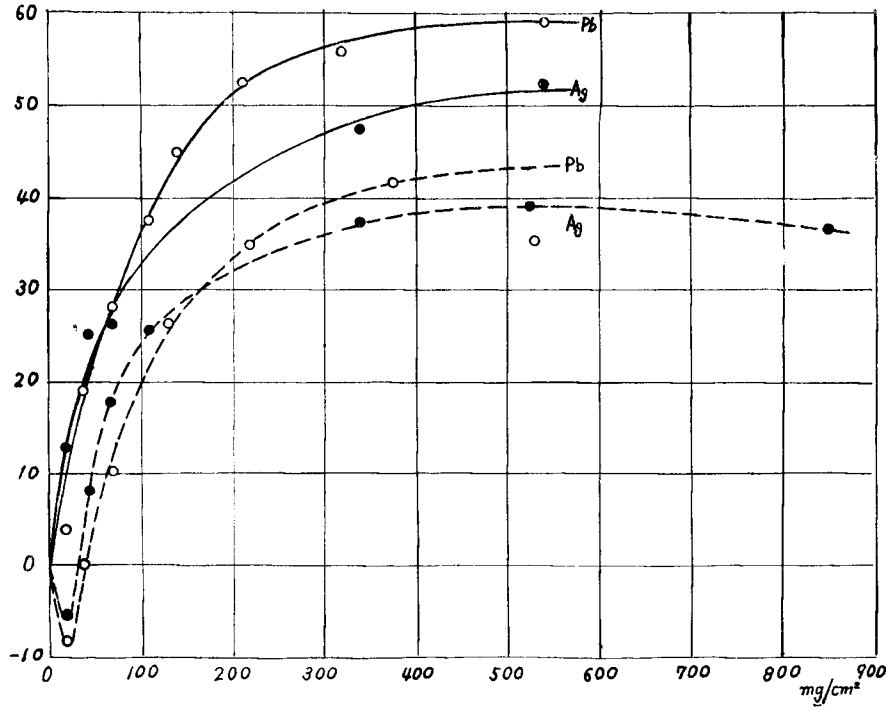

Fig. 5. Relations between the intensity of emergent electrons and the thickness of silver and lead scatterers at the scattering angle 0°. The ordinate is in the arbitrary scale.

$$I = I_\infty \frac{\cos\theta}{\mu}\left(1 - e^{-\mu \frac{x}{\cos\theta}}\right),$$

then we obtained the following μ's:

scattering angle θ	μ for lead (cm^2/mg)	μ for silver (cm^2/mg)
0°	0.0092	0.0124
25°	0.0067	
45°	0.0085	0.0086
65°	0.0047	0.0048
115°	0.0055	0.0058
135°		0.0076

In the case of the forward scattering the saturation thickness (the thickness where the intensity of the emergent electrons reaches 90% of the saturation value) decreases as the scattering angle increases. The decrease is slower than in the case of the self-scattering of β-rays where it is proportional to $\cos\theta$. It is quite natural that there is a large difference between the saturation thickness of the forward scattering

($\theta < 90°$) and that of the backward scattering ($\theta > 90°$). It is interesting to note that the shape of the curve of $\theta = 135°$ for lead is remarkably different from others. In Fig. 5, the dotted curves represent the intensity when the magnetic field is removed. In this case the electrons ejected from the container of the source and the layer of the air are mixed in the incident γ-ray beam. These electrons are absorbed in the sample, while the γ-ray ejects secondary electrons from it. When the sample is thin, the absorption of the incident electrons is dominant and the counting rate of the detector decreases with the thickness of the sample and the intensity curve has the negative value. When the sample is thick enough, all incident electrons are absorbed and the counting rate is governed only by the secondary electrons; and the intensitiy increases with the thickness of the sample and the shape of the curve becomes the same as in the case where the incident ray is not mixed with the electrons.

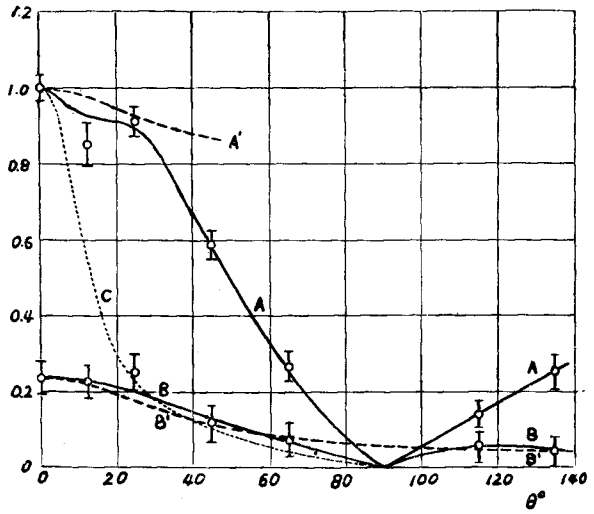

Fig. 6. Angular distributions of emergent electrons.
Curve A : Experimental value for the lead scatterer of 220 mg/cm² in thickness.
Curve B : Experimental value for the lead scatterer of 19.1 mg/cm² in thickness.
Curve A′: Calculated value for the lead scatterer of 220 mg/cm² in thickness.
Curve B′: Calculated value for the lead scatterer of 19.1 mg/cm² in thickness.
Curve C : Angular distribution of the Compton recoil electron.

Fig. 6 shows the results of the measurement of the angular distribution of emergent electrons from the scatterers. The curve A represents the results for the lead scatterer of 220 mg/cm² in thickness and the curve B represents that of 19.1 mg/cm². At $\theta = 12.5°$, the γ-ray beam struck directly the wall of the counter and we had to take a long measuring time. Therefore, considering the variation of the characteristics of the instrument during the measurement, the error at this angle might be larger than the statistical error shown in the figure.

Comparing these curves with the curve C which represents the angular distribution of the Compton recoil electron, the flat part of the curve A and B is remarkable. This is conceivable as the result of multiple scattering of the recoil electrons in the scatterer. In order to verify this effect, we calculated roughly the angular distribution

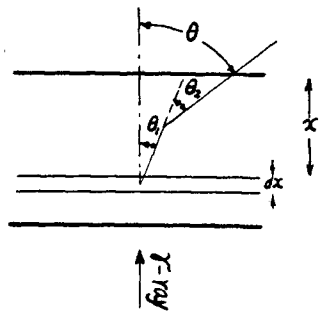

Fig. 7.

of the emergent electrons as follows.

We took the recoil electron to the direction θ_1 in dx and put its distribution as $\sigma(\theta_1)\sin\theta_1 d\theta_1 d\varphi_1$, as shown in Fig. 7. These electrons go out of the scatterer after passing the distance t. The direction of emerging electrons, however, is different from θ_1 as they perform multiple scattering on their way out. If this variation of direction is denoted by θ_2 and take the distribution at θ_2 as $f(\theta_2, t)\,d\theta_2$, the angular distribution of the emergent electrons becomes

$$I(\theta)\sin\theta\,d\theta d\varphi = \int_0^x dx \int_0^{\pi}\int_0^{2\pi} \sin\theta_1 d\theta_1 d\varphi_1 \cdot \sigma(\theta_1) f(\theta_2, t)\sin\theta\,d\theta d\varphi \qquad (1)$$

where

$$\cos\theta_2 = \cos\theta\cos\theta_1 + \sin\theta\sin\theta_1\cos(\varphi-\varphi_1)\,.$$

Various expressions of the distribution of multiple scattered electron have been presented by many authors, but we used the theory of S. Goudsmit and J. L. Saunderson[6] because it is rigourous and its analytical formulae are easy to handle. Putting $t = x/\cos\theta_1$,

$$f(\theta_2, t) = \frac{1}{4\pi}\sum_{n=0}^{\infty}(2n+1)\,G_n \cdot P_n(\cos\theta_2) \qquad (2)$$

$$\left.\begin{aligned} G_n &= \exp\left\{-2\pi\kappa^2 Ntn(n+1)\left[\log\xi - \left(\frac{1}{2}+\frac{1}{3}+\cdots+\frac{1}{n}\right)\right]\right\} \\ \kappa &= \frac{Ze^2}{mc^2}\,\frac{\sqrt{1-\beta^2}}{\beta^2}, \qquad \log\xi = \log\left(\frac{1.10 a_0}{\lambda\!\!\!^{-}}\,Z^{-1/3}\right) \end{aligned}\right\} \qquad (3)$$

where a_0 is the classical electronic radius, $\lambda\!\!\!^{-}$ is the wave length of the electron and N and Z has their usual meanings. By use of the relation

$$P_n(\cos\theta_2) = P_n(\cos\theta)\,P_n(\cos\theta_1) + 2\sum_{m=1}^{\infty}\frac{(n-m)!}{(n+m)!}P_n^m(\cos\theta)\,P_n^m(\cos\theta_1)\cos m(\varphi-\varphi_1)\,,$$

$I(\theta)$ is expressed as follows:

$$\left.\begin{aligned} I(\theta) &= \frac{1}{2}\sum_{n=0}^{\infty} a_n P_n(\cos\theta) \\ a_n &= (2n+1)\int_0^x dx \int_0^{\pi} P_n(\cos\theta_1)\,\sigma(\theta_1)\,G_n \cdot \sin\theta_1\,d\theta_1 \end{aligned}\right\} \qquad (4)$$

Integrating it with x, a's become

$$\left.\begin{aligned} a_0 &= \frac{1}{2\pi}\, x \cdot {}_e\sigma \\ a_n &= (2n+1)\int_0^{\pi/2} P_n(\cos\theta_1)\,\sigma(\theta_1)\Big[1-\exp\Big\{-2\pi\kappa^2 N\frac{x}{\cos\theta_1}\,n(n+1)\Big[\log\xi- \\ &\quad -\Big(\frac{1}{2}+\frac{1}{3}+\cdots+\frac{1}{n}\Big)\Big]\Big\}\Big]\sin\theta_1\cos\theta_1\,d\theta_1 d\varphi_1/2\pi\kappa^2 Nn(n+1)\Big[\log\xi- \\ &\quad -\Big(\frac{1}{2}+\frac{1}{3}+\cdots+\frac{1}{n}\Big)\Big] \qquad \text{for} \quad n\neq 0 \end{aligned}\right\} \quad (5)$$

where

$${}_e\sigma = \int_0^{\pi/2} \sigma(\theta_1)\sin\theta_1\,d\theta_1 .$$

For simplicity we assumed the interaction of the γ-ray with the scatterer is only with the Compton effect. This assumption does not affect essentially the result of this calculation as the cross-section of the photoelectric effect, in the case of lead, is less than 20% of the Compton effect. By integrating (5) numerically[7] and summing (4) up to $n=7$ we obtained the curve A′ and B′ of Fig. 6.

This calculation is based on various approximations. They do not hold when scattering angle is large, especially for the thick scatterer. For this reason the curve A′ and B′ have their meanings only when the scatterer is thin or the scattering angle is small. Comparing the curve A′ and B′ with the experimental results A and B, the consistency is rather good and the flattening of the top of the curves are well shown.

II. 2π-Forward and 2π-Backward Scattering

Experimental Procedure

For the purpose of measuring the intensity of the electrons which emerge forward and backward within a solid angle 2π, we produced a drum-shaped *G-M* counter which is shown in Fig. 8. The counter is 49.5 mm long and has a wall of aluminium of 0.2 mm thick and the cathode of 26.5 mm inner diameter. The thickness of the mica window of both sides is 7 mg/cm^2. The background counting rate is small because the collimated γ-ray beam pass through the counter without striking the wall. Since the scatterer is put close to a window of the counter as shown in the figure, we are able to count the electrons scattered within a solid angle of about 1.3π steradian.

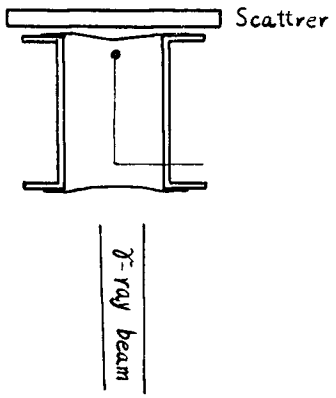

Fig. 8. Schematic drawing of the apparatus to measure 2π-forward and backward scattering.
This direction of the incident beam is at the case of the measurement of the backward scattering.

We measured the relation of the intensity of 2π-scattered electrons with the thickness of the scatterer and obtained the results as shown in Fig. 9 and Fig. 10. The saturation thickness are 270 mg/cm^2 for the forward scattering and 190 mg/cm^2 for the backward scattering, and they are quite uniform regardless of the kind of scatterer. These curves were not influenced at all when the magnetic field was removed.

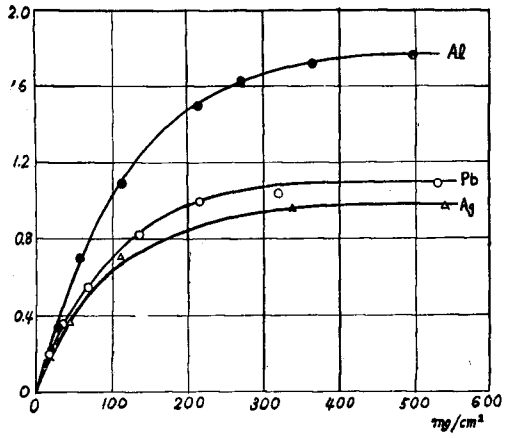

Fig. 9. Relations between the intensity of 2π-forward scattering electrons and the thickness of the scatterers of various elements. The ordinate is in the arbitrary scale.

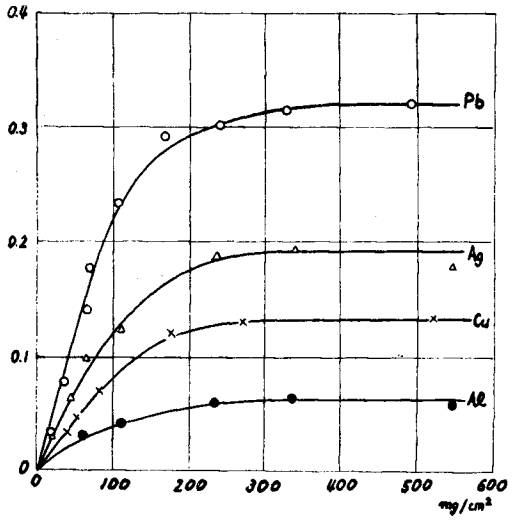

Fig. 10. Relations between the intensity of 2π-backward scattering electrons and the thickness of the scatterers of various elements. The ordinate is in the same scale as Fig. 9.

Relations of the saturation values of the intensity of the scattered electrons with the atomic number Z of the scattering materials are shown in Fig. 11. In the case of the backward scattering, saturation values are proportional to Z and this is similar to the Z-dependency of the β-ray of about 0.1 Mev.[5] G. J. Hine had carried out similar measurement employing his integration ionization chamber and he obtained the ratio of the intensity of the backward scattering to that of the forward scattering twice or thrice greater than that of ours. However, this is thought to be quite reasonable

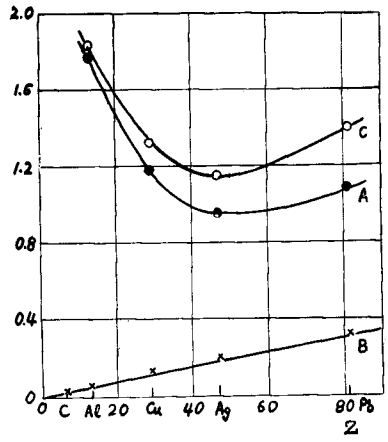

Fig. 11. The Z-dependency of the intensity of the scattering electrons.
Curve A: 2π-forward scattering
Curve B: 2π-backward scattering
Curve C: 4π-scattering

considering that the average energy of the backward scattering electrons is about 0.1 Mev. as has been discussed above and the specific ionization of these electron is larger than that of forward scattering electrons. The curve C in Fig. 11 shows the total intensity of the emergent electrons (forward scattering plus backward scattering), and it is conceivable that it expresses the γ-ray efficiency of the counter which have the walls of given materials.

The Z-dependency of the efficiency of G-M counter for γ-rays was measured by some workers. Our results are quite consistent with those of Norling,[2] but the data of Bradt *et al.*[3] are somewhat different from ours. Bradt *et al.* measured the energy dependence of the efficiency of aluminium, brass and lead cylindrical counters and their data showed that the efficiency of lead counter at the energy of 1.2 Mev. is larger than that of aluminium counter. On the contrary, our results showed that the aluminium counter has a larger efficiency for the γ-rays of Co^{60} than the lead counter. This discrepancy might have been caused by the fact that they used the counter of cylindrical type whereas our measurements are equivalent to use the rectangular counter. However, they did not measure in the neighborhood of 1.2 Mev. but they had simply interpolated the curves between 0.5 Mev. and 2.6 Mev.

Theoretical calculation of the efficiency of the G-M counter for γ-ray was done by von Droste[9] quite long ago and his methods are still used today. By his expression the efficiency is

$$\varepsilon = 2k(\tau R_\tau + \sigma \bar{R}_\sigma + 2\kappa \bar{R}_\kappa)$$

where τ, σ and κ is the cross-section of the photoelectric effect, the Compton effect and the pair production, and R's are the ranges of the electrons ejected by each process, k is the probability of the secondary electron jumping into the counter and it depends on the initial distribution of the electrons. He assumed a cubically symmetric distribution of emergent electrons and obtained $k = 1/4$.

This assumption is correct for the low energy region. But as the energy of the γ-ray becomes higher, the approximation becomes unsatisfactory. In the neighborhood of 1.2 Mev., the initial distribution of the electrons deviates from the cubic symmetry and the effect of their multiple scattering becomes very large. We will show that, when the multiple scattering is taken into consideration, the value of k becomes small when the atomic number Z of a substance on the wall is large.

Let us take a G-M counter with rectangular cross-section and let the γ-ray penetrate perpendicularly on the wall. We neglect the electrons entering from the backside wall of the counter. This neglection of the backward scatrering is permissible according to the results of our experiment. We assume also that the secondary electrons are ejected only to the same direction as γ-ray. This assumption is closer to the reality than the assumption of cubically symmetric distribution for the energy

of 1.2 Mev. After the secondary electrons passed the distance x in the scatterer, the probability that their direction is within the cone, of half angle θ_0 is

$$\int_0^{\theta_0} \frac{2}{\alpha^2}\theta\, e^{-\theta^2/\alpha^2}\, d\theta \tag{6}$$

where

$$\alpha^2 = \frac{8\pi NZ(Z+1)\, e^4}{p^2v^2}\, x \log\left[4\pi Z^{4/3}Nx\left(\frac{\lambda}{mv}\right)^2\right] \tag{7}$$

If we approximate $\frac{Z}{A}\approx\frac{1}{2}$ and neglect the variation of the logarithmic part,

$$k\approx\int_0^R dx\int_0^{\cos^{-1}\frac{x}{R}} \frac{1}{bzx}\, e^{-\frac{\theta^2}{bZx}}\,\theta d\theta \tag{8}$$

where b is a constant and R is the range of the secondary electrons. Integrating (8), we obtain

$$k\approx -\frac{1}{bZ}\, E_i\left(-\frac{2}{bZR}\right) \tag{9}$$

where E_i is the exponential integral. For the secondary electrons of the γ-ray of 1.2 Mev., $\frac{2}{bR}\approx 10$. By use of this value

$$\frac{2}{R}\, k = 0.25,\ 0.27,\ 0.25 \quad \text{and} \quad 0.20$$

for aluminium, copper, silver and lead respectively. Thus, we obtained the result that the efficiency became smaller for the heavy elements than that obtained by von Droste.

III. Conclusion

From these results, it became obvious that the scattering of the electrons has the most important meaning in discussing the behavior of the secondary electrons of the γ-ray of 1.2 Mev. in various substances. In this energy region, the approximation of the complete diffusion of the electron and of the neglection of its scattering are not adequate.

It became obvious also that the efficiency of the G-M counter for the γ-rays of Co^{60} can be smaller for the heavy element than the value calculated by von Droste by a factor which depends on Z of the wall material. But we cannot determine which is more efficient, the lead counter or the aluminium counter, in the case of cylindrical type, as we are not yet tested experimentally.

However, the truth of the traditional belief that the counter, whose wall consists of a heavy element, has a larger efficiency, is doubtful when the energy of the γ-ray is about 1.2 Mev.

Authors wish to express their sincere thanks to Mr. I. Kumabe for his helpful advice pertaining to the experimental apparatus and his valuable discussions on the results.

References

1) Kikuchi, Aoki and Fushimi: Proc. Phys.-Math. Soc. Japan, **18**, 727 (1936).
2) F. Norling: Phys. Rev., **58**, 277(L) (1940).
3) H. L. Bradt, P. C. Gugelot, O. Huber, H. Medicus, P. Preiswerk and P. Scherrer: Helv. Phys. Acta., **19**, 77 (1946).
4) E. T. Jurney and F. Mainenshein: R. S. I., **20**, 932 (1949).
5) H. H. Seliger: Phys. Rev., **78**, 491 (1950), **88**, 408 (1952).
I. Kumabe and S. Shimizu: Bulletin of Institute for Chemical Research, Kyoto Univ., **32**, 183 (1955).
6) S. Goudsmidt and J. L. Saunderson: Phys. Rev., **57**, 24 (1940).
7) A. T. Nelm: Natl. Bur. Stands. Circular No. 542.
8) G. J. Hine: Nucleonics, **10**, No. 1, 11 (1952).
9) von Droste: Zeits. für Phys., **100**, 529 (1936).